Demonstration of an all-diode pumped soft x-ray laser and other advances in table-top soft x-ray lasers

Jorge J. Rocca[1,2], B. Reagan[1], F. Furch[1,2], Y. Wang[1], D. Alessi[1], D. H. Martz[1], M. Berrill[1], V.N. Shlyaptsev[1], B. M. Luther[1], A. H. Curtis[1]
rocca@engr.colostate.edu

[1]NSF ERC for Extreme Ultraviolet Science and Technology and Department of Electrical and Computer Engineering, Colorado State University, Fort Collins, Colorado 80523, USA
[2] Department of Physics, Colorado State University, Fort Collins, Colorado 80523, USA

Abstract. We report the first demonstration of an all-diode-pumped soft x-ray laser system. Lasing was achieved in the λ = 18.9 nm line of Ni-like Mo ions pumping with a diode-pumped cryo-cooled Yb:YAG chirped-pulse-amplification laser system that generates 1 J pulses of 8.5 ps duration. Driver lasers pump by diodes opens the possibility to develop a new generation more compact soft x-ray lasers operating at significantly increased repetition rates for applications.

In a separate development we have demonstrated a gain-saturated table-top λ=10.9 nm laser operating at 1 Hz repetition rate with an average power of 1 μW in the $4d^1S_0 \rightarrow 4p^1P_1$ transition of nickel-like Te and observed lasing at 8.8 nm in nickel-like La in plasmas exited by a Ti:sapphire laser. Utilizing the same pump laser we obtained laser pulse energies of up to 10 μJ and an average power of 20 μW in the 13.9 nm line of Ni-like Ag.

In a third set of experiments we characterized the beam properties of an injection-seeded soft x-ray laser based on the amplification of high harmonic pulses in a solid-target plasma soft x-ray laser amplifier. Injection-seeding is shown to dramatically improve the far-field laser beam profile and reduce the beam divergence. Measurements and 2-dimensional simulations for a 13.9 nm nickel-like Ag amplifier show that the amplified beam divergence depends strongly on the seed divergence, and can therefore be tailored by selecting it.

1. Demonstration of a Diode-pumped soft x-ray laser

The development of high average power soft x-ray lasers (SXRL) is interesting for a number of applications. As summarized below in Section 2, gain-saturated table-top soft x-ray lasers pumped by infrared chirped pulse amplification (CPA) laser systems have been demonstrated at wavelengths down to 10.9 nm [1], and with average powers up to 20 μW at 13.9 nm [2]. However the repetition rate and therefore the average power of these flashlamp-pumped lasers is typically limited to less than 10 Hz. The small quantum defect of Yb doped materials and the high pumping efficiency that

J. Lee et al. (eds.), *X-Ray Lasers 2010,* Springer Proceedings in Physics 136,
DOI 10.1007/978-94-007-1186-0_7, © Canopus Academic Publishing Limited 2011

results from pumping with a narrow bandwidth source of the optimum wavelength allow for the development of solid state laser systems that are significantly more compact. Additionally, when cooled to cryogenic temperature the thermal conductivity increases nearly an order of magnitude and the saturation fluence decreases by a factor of 7 allowing efficient operation at very high average powers.

Herein we discuss the demonstration of a table-top SXRL pumped by very compact all diode pumped CPA laser system based on cryogenically-cooled Yb:YAG amplifiers [3]. The pump laser produces 1 J, picosecond pulses at 10 Hz repetition rate. To the best of our knowledge this is the highest energy demonstrated to date for a diode-pumped system producing sub-10 ps pulses. A block diagram of the CPA system is illustrated in Fig.1. The system consists of a modelocked oscillator, pulse stretchers, two stages of amplification and a grating pulse compressor. The SXRL system is completed with a focusing optics chamber and the target chamber. The entire laser system with the exception of the pulse compressor fits onto a single standard 12'x5' optical table. The pump laser system consists of a SESAM modelocked Yb:KYW oscillator pumped by a 30 W, 980 nm, laser diode, two grating stretchers (only one shown in schematic of Fig.1) , a regenerative amplifier, a cryo-cooled Yb:YAG amplifier and a dielectric grating compressor. The laser oscillator produces a 1.2 W train of 300 fs pulses at a repetition rate of 57 MHz. The beam exiting the oscillator is split into three

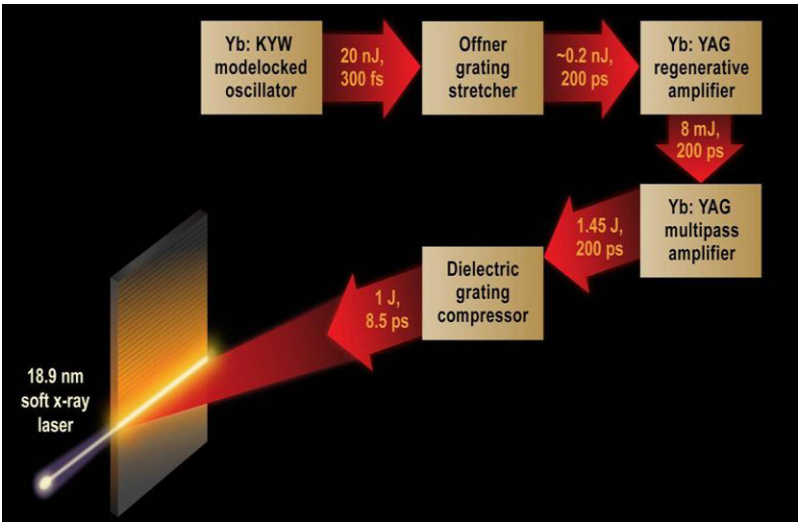

Fig. 1: Schematic Block diagram of the diode pumped soft x-ray laser system.

pulses and sent through two different grating stretchers before being recombined into a single beam to create a train of two 160 ps pulses with negative group velocity dispersion (GVD) and a 200 ps pulse with positive

GVD. These stretched pulses are subsequently amplified in two cryo-cooled Yb:YAG amplifiers. The first amplifier is a regenerative amplifier pumped by a 90 W fiber-coupled laser diode emitting at 940 nm. The cavity of the regenerative amplifier ensures that the three stretched pulses are collinear throughout the system. The regenerative amplifier boosts the pulse energy to ~ 7 mJ. The regenerative amplifier was demonstrated to maintain the pulse energy and beam quality at repetition rates up to 100 Hz (Fig.2).

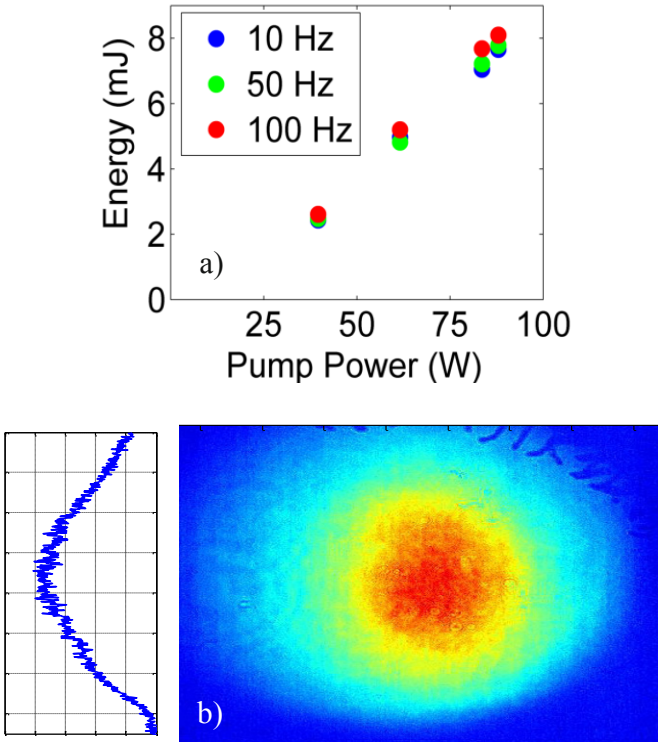

Fig. 2. a) Output pulse energy of the cryo-cooled Yb:YAG regenerative amplifier as a function of diode pump power for three repetition rates. b) Output beam profile.

The second amplification stage, shown in Fig. 3, consists of a 12-pass multipass amplifier which utilizes to two cryo-cooled, Yb:YAG disks in the active mirror configuration. Each crystal is pumped by a 3.5 kW diode stacks producing 2 ms pulses . This stage amplifies the pulses to energies of 1.45 J at 10 Hz repetition rate (Fig 3b). Following amplification, the pulses are compressed by a 70 % efficient dielectric grating pair to produce 8.5 ps duration 1 J pulses.

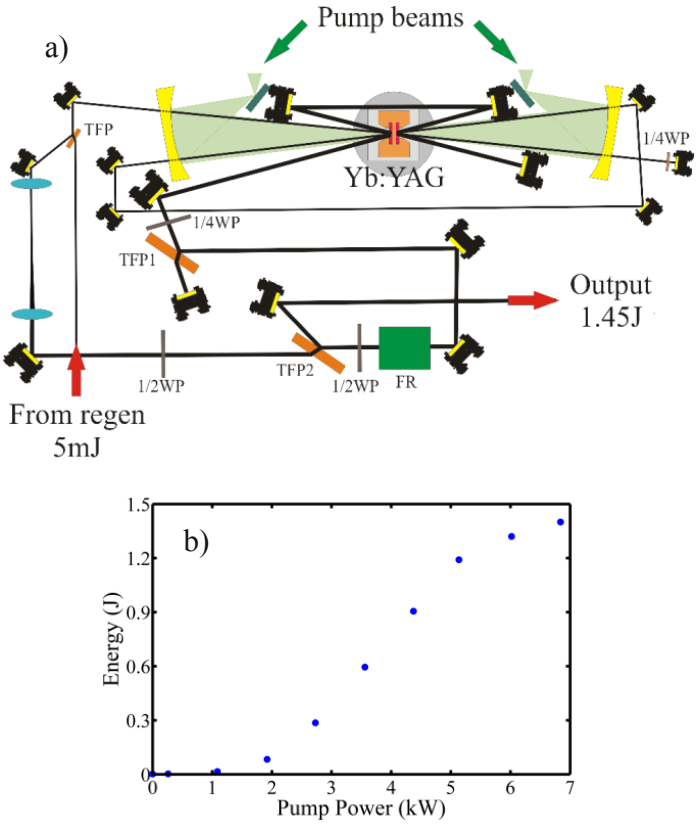

Fig. 3: a) Schematic layout of the 12-pass Yb:YAG cryocooled amplifier. WP = waveplate; TFP = Thin Film Polarizer; FR = Faraday Rotator . b) Output pulse energy of the Yb:YAG amplifiers as a function of diode pump power. The data was obtained at 10 Hz repetition rate.

The all-diode-pumped CPA laser described above was used to pump a λ=18.9 nm soft x-ray laser. The train of pulses generated by the pump laser was focused at grazing incidence onto a Mo target [4,5] to form a 4mm long by 35 μm wide line. Two pre-pulses with 350 ps FWHM duration create and ionize the plasma that is subsequently rapidly heated by a 8.5 ps FWHM pulse to produce a transient population inversion in the 18.9 nm transition of Ni-like Mo ions. Figure 4 (a) shows a single shot on-axis spectrum corresponding to a plasma create by focusing 700 mJ of total pump energy incident on target. The intensity of the 18.9 nm Ni-like Mo laser line is similar to that of other plasma lines. Increasing the pump energy to 940 mJ results in dramatic growth of the laser line intensity, accompanied by a significant angular narrowing of the line, a clear evidence of strong laser amplification (Fig. 4 (b)). This new type of compact diode-pumped SXRLs will be capable to operate at greatly increase repetition rates, producing high average power for applications.

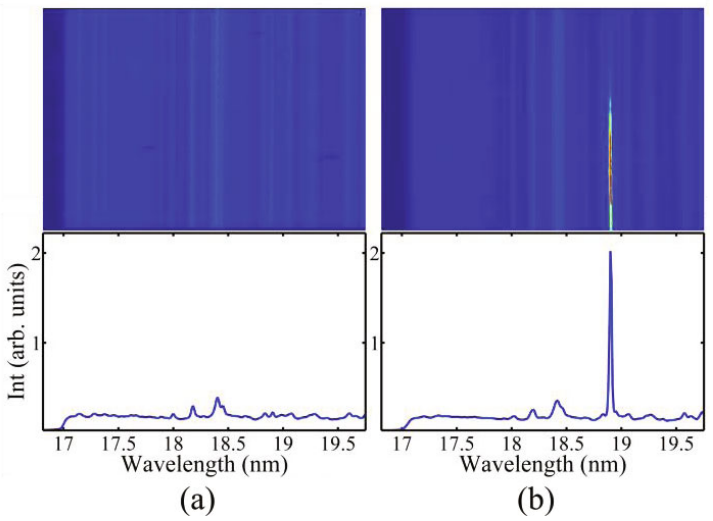

Fig. 4. Soft x-ray spectra of a molybdenum plasma heated by the diode pumped Yb:YAG CPA laser system (a) On-axis soft x-ray spectrum taken with a total pump energy on target of 0.7 J. (b) The same spectrum taken with 0.94 J of pump energy, showing laser amplification in the 18.9 nm laser line of Ni-like Mo.

2. Gain-saturated 10.9 nm SXRL at 1 Hz repetition rate and lasing at 8.8 nm.

There is also interest in extending table-top SXRLs to shorter wavelengths. However, the steep wavelength scaling of the energy necessary to pump such lasers imposes a challenge to the demonstration of gain-saturated high repetition rate lasers at shorter wavelengths. As a result, the use of table-top SXRLs in applications has been limited to wavelengths above 13.2 nm [6,7]. We have recently demonstrated a gain-saturated table-top 10.9 nm laser in the $4d^1S_0 \rightarrow 4p^1P_1$ transition of nickel-like Te that operates at 1 Hz repetition rate. Lasing in nickel-like Te was first demonstrated using 520 J of optical laser pump energy to heat a collisionally pumped plasma [8]. More recently gain in this transition was obtained in a table-top set up using ~ 1 J pulses of 8 ps duration impinging at a grazing angle of 23 degrees to heat a pre-created plasma [9]. However, the output laser intensity was far from saturation, producing an insufficient photon flux for applications.

Gain-saturated lasing was generated by rapidly heating a 5 mm wide solid Te slab target using a CPA Ti:sapphire laser system that produces λ = 800nm pulses with energies up to 5.5 J before compression. After the third amplification stage the stretched pulses have a duration of 210 ps. A beam

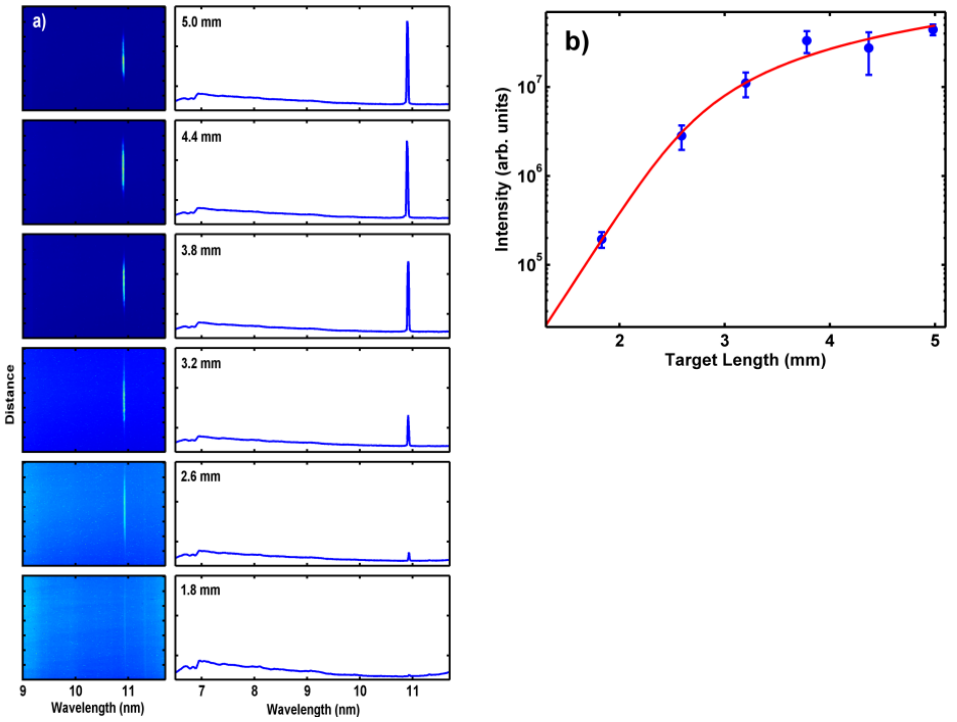

Fig. 5. a) On axis single-shot spectra from the Te plasma for increasing plasma column up to 5 mm. Strong lasing is observed at 10.9 nm. b) Measured laser line intensity as a function of plasma column length. Each data point is an average of eight laser shots.

splitter placed after the final amplification stage was used to re-direct 40% of the energy into a pre-pulse arm used to create a plasma with relatively smooth density gradients. Two pre-pulses pulses were focused into a 30 μm x 5 mm FWHM line onto the target. The remaining 60% of the energy was compressed into a 5 ps FWHM pulse and was focused at 30 degrees grazing incidence into an overlapping line of the same dimension.

Figure 5a shows a series of on-axis single-shot spectra and their corresponding vertical integrations for plasmas of different lengths between L = 1.8 and 5 mm. The total pump energy on target was fixed at 3.4 J. The SXRL intensity rapidly grows with target length to dominate the entire spectra, eventually reaching saturation. From these spectra it was determined that for the 5 mm target the SXRL beam divergence in the direction parallel to the target is 8.5 ± 1 mrad. The measured SXRL intensity as a function of target length is shown in Fig. 5b. The fit shows a small signal gain of g_0= 45.3 cm^{-1} and an integrated gain length product of 14.1 at 5 mm. At about 3 mm, the intensity starts to show signs of saturation. Strong soft x-ray lasing was observed to take place over a relatively narrow range of excitation delays centered at 200 ps. Lasing is observed to cease when the delay is increased to

400 ps. However, further increase of the delay results in weak lasing around 550 ps. This late laser pulse, predicted by the simulations, occurs when Co-like ions recombine into Ni-like ions, indicating the plasma is slightly over-ionized at the time of peak laser gain. A SXRL average power of ~ 1 μW was obtained pumping a 6 mm wide Te target with 4.2 J of total laser pump energy on target at a repetition rate of 1 Hz. The most intense laser pulses reach an energy of ~ 2 μJ. Assuming a laser pulse duration of 4 – 5 ps and a near-field laser spot ~ 15 μm in diameter from 3-D post processor ray trace simulation to a 1.5 D hydrodynamic/atomic physics simulation, the laser beam intensity is estimated to reach an intensity of ~ 2.5×10^{11} Wcm^{-2}. This intensity exceeds the 0.6-1.4×10^{10} Wcm^{-2} computed saturation intensity of this line for the plasma conditions of the experiment. This is the shortest wavelength gain-saturated table-top laser reported to date.

Using a sequence of Ti:sapphire laser pulses with a total energy of 5.2 J to heat a lanthanum target lasing was observed in the $4d^1S_0 \rightarrow 4p^1P_1$ transition of nickel-like La. Fig.6 is a single shot on-axis spectra of the lanthanum plasma showing amplification at 8.8 nm in this transition.

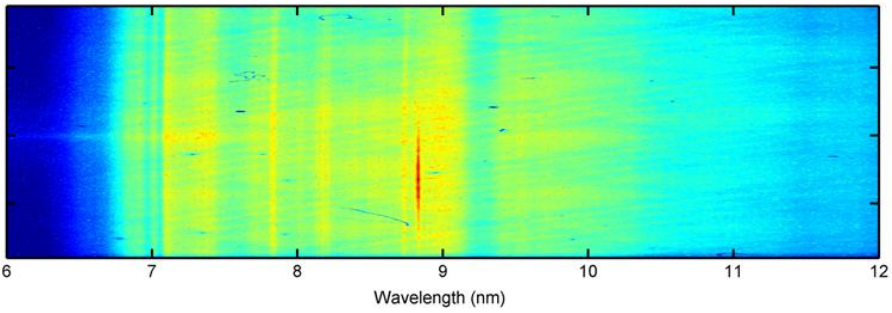

Fig.6. On axis spectra of a lanthanum plasma column showing lasing in the 8.8 nm line of nickel-like La.

3. Demonstration of high pulse energy 13.9 nm laser at 2.5 Hz repetition rate

Table-top SXRLs with wavelengths in the 13 nm spectral region have produced picosecond laser pulses with energy of ~1 μJ and average powers up to 2 μW when operating at 5-10 Hz repetition rate [9,10]. Significantly larger SXRL pulse energies, of ~10-25 μJ at a rate of one laser shot every several minutes have been produced using more energetic pump lasers [11,12]. We have recently obtained a significant increase in laser pulse energy of muti-Hz table top SXRL in the 13 nm spectral region by demonstrating a table-top

laser that is capable of producing laser pulses with average energy of 7 μJ at 2.5 Hz repetition rate at 13.9 nm [2]. With an average power of ~20 μW this laser will make possible new applications of coherent soft x-ray light on a table-top.

The SXRL pulses are generated in a narrow line focus Ag plasma heated by a sequence of pulses generated by a CPA Ti:Sapphire laser consisting of a Kerr mode-locked laser oscillator and three stages of amplification. The third amplification stage is pumped by a high energy frequency-doubled Nd-glass slab laser developed in house, designed operate at a repetition rates of a few Hz (Fig. 7). The front end of this pump laser consists of a Q-switched Nd:YLF oscillator that is subsequently amplified in two double-pass Nd:YLF rods. The output of the pre-amplifier is split into two beam and each of them is amplified by 8 passes thought a flash-lamp pumped Nd:glass slab amplifier (Fig 1.b). The output of each arm is frequency doubled in a KDP crystal to produce up to 10 J of 532 nm light, which is relay imaged into the third stage Ti:sapphire amplifier rod to produce λ=800 nm laser pulses with up to 7.5 J energy at 2.5 Hz repetition rate.

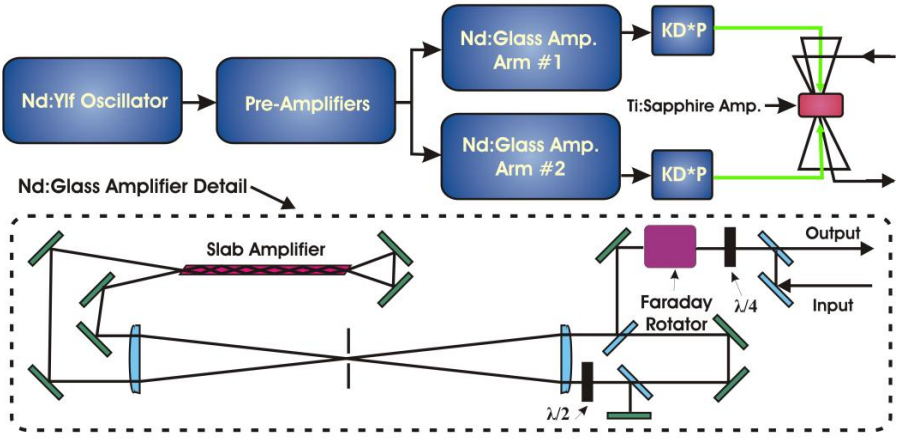

Fig.7. Block diagram of the third amplification stage of the Ti:sapphire laser used to pump the SXRL.

SXRL experiments at 13.9 nm were conducted by focusing up to 4.9 J of Ti:Sapphire laser energy into a line focus ~30 μm wide and 6.3 mm in length on the surface of a Ag slab target. Part of the output energy from the third amplification stage is directed to a pre-pulse arm using a 40% beam splitter. The rest of the energy was compressed to 6 ps in a vacuum compressor using dielectric gratings. Pre-pulses of 210 ps duration with a total energy of ~2.2 J were directed at normal incidence onto the target to create a Ag plasma that subsequently is rapidly heated by a 6 ps pulse impinging at 23 degree grazing incidence. A highly saturated SXRL beam results. The rapid heating of the

plasma to electron temperatures of up to ~ 550 eV generates a transient population inversion and amplification in the λ = 13.9 nm $4d^1S_0 \rightarrow 4p^1P_1$ transition of nickel-like Ag. The laser emits a single highly monochromatic line at 13.9 nm. Figure 8 shows the shot-to-shot variation of the laser output pulse energy when the laser is operated at 2.5 Hz repetition rate. The most energetic pulses exceed 8 μJ and the average power

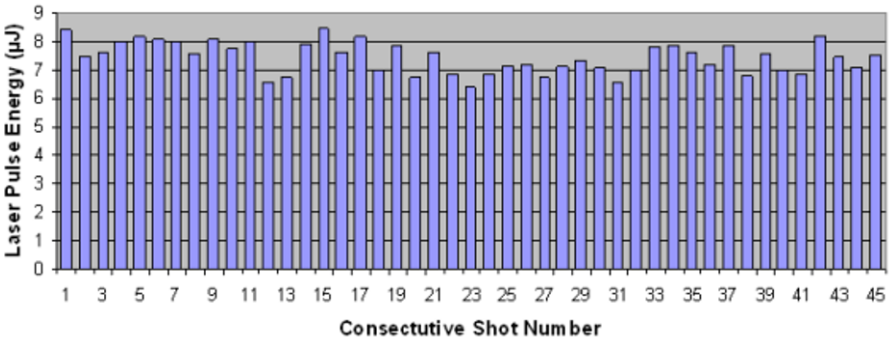

Fig. 8. Laser pulse energy output of the 13.9 nm laser when operated at 2.5 Hz repetition rate. The average power is ~ 20 μW and the shot-to-shot laser pulse energy variation is σ = 7 %.

approaches 20μW. The average pulse energy is 7.4 μJ and the shot-to-shot energy variation is characterized by a standard deviation of 7%. This relatively high shot-to-shot laser energy stability for a plasma amplifier is the result of the highly saturated regime of operation of this soft x-ray laser amplifier.

4. Beam Characteristics of an Injection-Seeded Solid-Target Soft X-Ray laser

Injection-seeding of these ASE SXRL amplifiers with high harmonic pulses can produce intense SXRLs with full spatial and temporal coherence, shorter pulse duration, reduced divergence, near-gaussian spatial beam profiles, and defined polarization [13-18]. We summarize results of the recent characterization of the near-field and far-field spatial distribution and laser line profile of a seeded and self-seeded (ASE) solid target SXRL amplifier.

The experiments were conducted by seeding a nickel-like Ag SXRL amplifier (λ = 13.9 nm) with 59th harmonic pulses of a Ti:sapphire laser. A Ti:sapphire laser centered at 815nm was used to create and heat the plasma with a sequence of two pre-pulses followed by an ~0.9 J heating pulse of 6.7 ps duration impinging at a grazing incidence angle of 23°. The pump pulses were focused onto a 3 mm wide Ag target to form a 30 μm×4.1mm FWHM long line. A small portion of the pump laser energy was focused in a Ne gas jet to generate the high harmonic seed. The output of the gas jet was relay imaged onto a ~100 μm diameter spot at the input of the plasma amplifier

using a gold-coated toroidal mirror designed to operate at a grazing incidence angle of 10°. Figure 9 shows the measured far-field beam profile of the unseeded and seeded SXRL amplifier using a back illuminated CCD placed 0.86 m from the source. Injection seeding dramatically reduces the beam divergence and results in a nearly Gaussian far field profile (Fig. 9b).

Laser experiments were conducted using two different seed pulse divergences to study the dependence of the amplified beam on the seed. When a harmonic seed pulse with a FWHM divergence of 0.5±0.03 x 0.7±0.04 mrad in the directions perpendicular and parallel to the target respectively was used to seed the plasma, an amplified pulse with a divergence of 1.4±0.14 x 0.7±0.07 mrad was measured to result. Simulations agree in showing that the divergence of the amplified beam in the direction parallel to the target surface

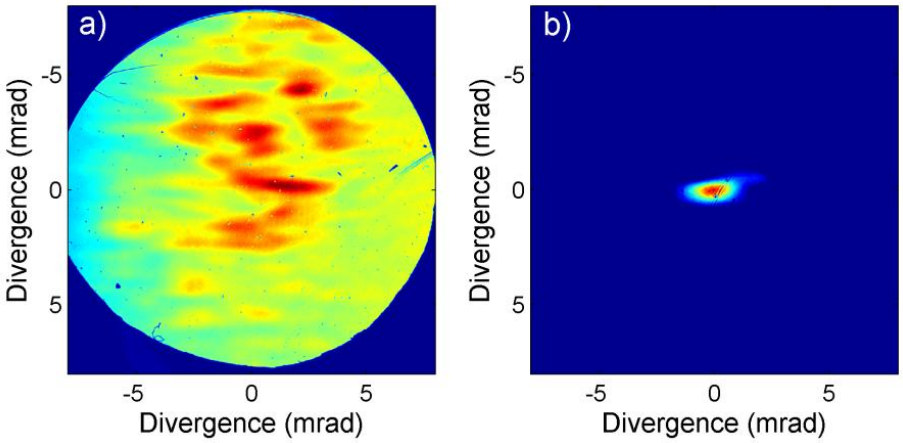

Fig. 9. Measured far-field distribution of an (a) self-seeded (ASE) and (b) seeded 13.9nm Ag solid-target SXR laser. The circular aperture in (a) is caused by the aperture of a thin-film filter.

closely resembles that of the seed beam, while the divergence perpendicular to the target surface is larger due to refraction [18]**.** When the divergence of the harmonic seed was increased to 1.6±0.3 x 1.4±0.4 mrad pulse, an amplified pulse with a divergence of 1.5±0.08 x 1.2±0.15 mrad was measured. The results show that when the divergence of the input harmonic seed is larger than ~1 mrad the far field of the amplified seed is almost completely dominated by the seed characteristics, while for smaller divergences it is controlled by both the input seed and refraction. These beam divergences are nearly an order of magnitude smaller than those corresponding to the unseeded amplifier. The near-field beam profiles of the self-seeded (Fig. 9a) and seeded (Fig. 9b) amplifier beams were measured using a 15.2x magnification imaging system. The measured near-field and far-field profiles were compared to simulations (Fig. 10). The location of the center of the near-field beam spot respect to the target surface, which is dominantly determined

by the position of the peak of the gain, was measured to be at a distance of 33±4 μm, in good agreement with the simulated near field profile. The near-field beam size of both the seeded and unseeded lasers is shown to be determined by the size of the gain region and the divergence of the amplified beams. The larger near-field spot size of the ASE laser in the direction parallel to the target surface is due to the larger divergence of the ASE laser, which allows rays with different trajectories to amplify across the entire gain region.

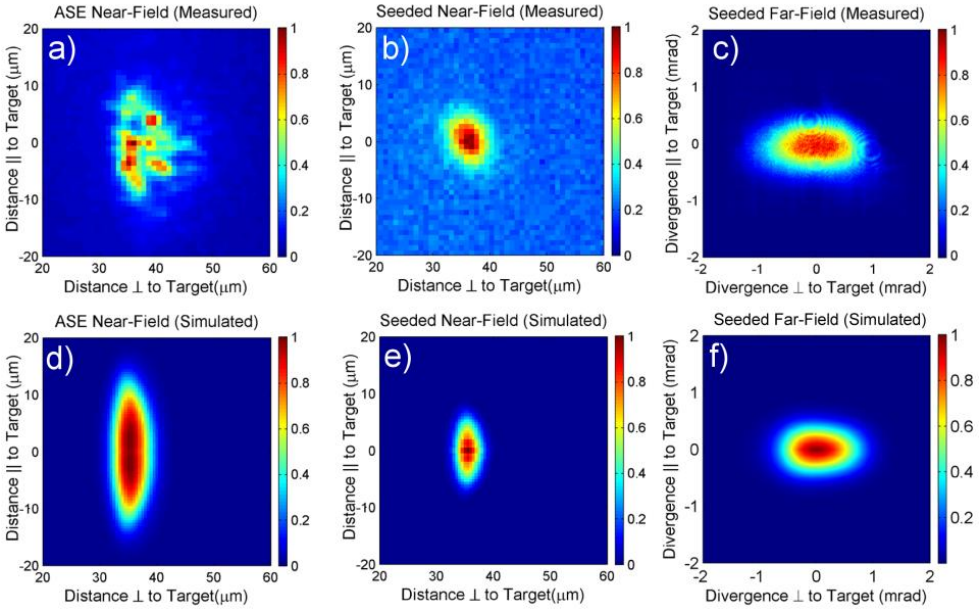

Fig. 10. Measured and simulated near field profiles of a self-seeded and seeded ASE amplifiers, and comparison of measured and simulated far-field profiles for the seeded laser.

Another paper in these proceedings discusses the results of the study of the temporal coherence of this type of injection-seeded solid-target amplifier utilizing a variable pass difference bi-mirror interferometer [19].

5. Acknowledgments

This work was sponsored by the NSF Engineering Research Center for Extreme Ultraviolet Science and Technology, award EEC-0310717, and the and by the Chemical Sciences, Geosciences and Biosciences Division, Office of Basic Energy Sciences, Office of Science, U.S. Department of Energy (DOE). M. B. acknowledges support from the Department of Energy (DOE) CSGF grant DEFG02-97ER25308.

6. References

1. D. Alessi, D.H. Martz, Y. Wang, M. Berrill, B.M. Luther, and J.J. Rocca, Opt. Lett. **35**, 414 (2010).
2. D. Martz, D. Alessi, B.M. Luther, Y. Wang, D. Kemp, M. Berrill, and J.J. Rocca, Opt. Lett. **35**, 1632 (2010).
3. F. Furch, B. Reagan, B. Luther, A. Curtis, S. Meehan and J.J. Rocca, Opt. Lett. **34**, 3352 (2009).
4. R. Keenan, J. Dunn, P. K. Patel, D. F. Price, R. F. Smith, and V. N. Shlyaptsev, Phys. Rev. Lett. **94**, 103901 (2005)
5. B. M. Luther, Y. Wang, M. A. Larotonda, D. Alessi, M. Berrill, M. C. Marconi, J. J. Rocca, and V. N. Shlyaptsev, Opt. Lett. **30**, 165-167 (2005)
6. G. Vaschenko et al., Opt. Lett. **31**, 1214 (2006).
7. F. Brizuela, S. Carbajo, A. Sakdinawat, D. Alessi, D.H. Martz, Y. Wang, B. Luther, K.A. Goldberg, I. Mochi, D. T. Attwood, B. La Fontaine, J.J. Rocca, and C.S. Menoni, Opt. Express, **18**, 14467 (2010).
8. H. Daido, S. Ninomiya, T. Imani, R. Kodama, M. Takagi, Y. Kato, K. Murai, J. Zhang, Y. You, and Y. Gu, Opt. Lett. **21**, 958-960 (1996).
9. Y. Wang, M.A. Larotonda, B.M. Luther, D. Alessi, M. Berrill, V.N. Shlyaptsev, Phys. Rev. A **72**, 053807 (2005).
10. H. T. Kim, I. W. Choi, N. Hafz, J. H. Sung, T. J. Yu, K. H. Hong, T. M. Jeong, Y. C. Noh, D. K. Ko, K. A. Janulewicz, J. Tümmler, P. V. Nickles, W. Sandner, and J. Lee, Phys. Rev. A 77, 023807 (2008).
11. J. Dunn, Y. Li, A. L. Osterheld, J. Nilsen, J. R. Hunter, and V. N. Shlyaptsev, Phys. Rev. Lett. **84**, 4834 (2000).
12. T. Kawachi, M. Kado, M. Tanaka, A. Sasaki, N. Hasegawa, A. V. Kilpio, S. Namba, K. Nagashima, P. Lu, K. Takahashi, H. Tang, R. Tai, M. Kishimoto, M. Koike, H. Daido, and Y. Kato, Phys. Rev. A **66**, 033815 (2002).
13. Ph. Zeitoun, et al., Nature **431**, 426 (2004).
14. Y. Wang, E. Granados, M.A. Larotonda, M. Berrill, B.M. Luther, D. Patel, C.S. Menoni, and J.J. Rocca, Physical Review Letters **97**, 123901 (2006).
15. Y. Wang, E. Granados, F. Pedaci, D. Alessi, B. Luther, M. Berrill, and J.J. Rocca, Nature Photonics **2**, 94 (2008).
16 Y. Wang, M. Berrill, F. Pedaci, M. M. Shakya, S. Gilbertson, Zenghu Chang, E. Granados, B. M. Luther, M. A. Larotonda, and J. J. Rocca, Phys. Rev. A **79**, 023810 (2009).
17 Kawachi, T. et al., Proc. SPIE **5919**, 155 (2005).
18 M. Berrill, D. Alessi, Y. Wang, S.R. Domingue, D.H. Martz, B. Luther, Y. Liu, and J. J. Rocca, Optics Lett. **35**, 2317 (2010).
19. A. Klisnick et al. in these Proceedings.